Academic Journal of Science and Technology
ISSN: 2771-3032 | Vol. 13, No. 2, 2024

Research on Vulnerability Assessment of Disaster Bearing Bodies Based on AHP-Cloud Model

Xushan Yuan[1, *]

[1]College of Disaster Prevention Science and Technology, School of Emergency Management, Sanhe 065201, China
[*]Corresponding: Yuan Xushan (2505475983@qq.com)

Abstract: This study selects 16 vulnerability indicators of meteorological disaster-bearing bodies in Yining County based on socio-economic data to construct a vulnerability assessment system for meteorological disaster-bearing bodies, including population vulnerability, economic vulnerability, and social vulnerability. The AHP-Cloud model is utilized to assign weights to each indicator, and the vulnerability and spatial-temporal distribution characteristics of the population-economy-society disaster-bearing bodies in Yi Ning County are evaluated and analyzed. The results show that (1) Demographic, economic, and social factors significantly affect the vulnerability of meteorological disaster-bearing bodies in Yi Ning County. High aging, young age, and population growth exacerbate vulnerability, while the economy, road network, and construction land affect social vulnerability. (2) The population vulnerability in Yi Ning County is influenced by topography, with low vulnerability in the north and high vulnerability in the south. The southern plains are highly vulnerable due to their high population density. From 2005 to 2020, population growth and aging exacerbated population vulnerability, and economic and social vulnerability exhibited similar spatial-temporal differences as population vulnerability. (3) Overall, the vulnerability of meteorological disaster-bearing bodies in Yi ning County is mainly dominated by population and economy. Towns and villages in the south have high vulnerability, and the overall trend is increasing. These conclusions can provide scientific evidence for relevant departments in Yi Ning County to reduce the vulnerability of meteorological disaster-bearing bodies and improve disaster prevention and mitigation capabilities.

Keywords: Analytic Hierarchy Process (AHP); Cloud Model; Meteorological Disaster; Vulnerability of Disaster-Bearing Bodies; Yi Ning County.

1. Introduction

Against the backdrop of rapid global population and economic growth, the frequency and severity of meteorological disasters are increasing. Natural geographical and climatic factors influence the formation of meteorological disasters in a region. It is closely related to the increasing number of disaster-bearing bodies and their vulnerability (Li et al., 2024). Vulnerability generally includes physical vulnerability and social vulnerability. Physical vulnerability refers to the average degree of destruction or loss of a disaster-bearing body under a certain intensity of hazard factors, representing the inherent attributes of the disaster-bearing body, i.e., the loss suffered by the disaster-bearing body is directly caused by the effect of hazard factors. Therefore, in evaluating physical vulnerability, the risk of hazard factors and the degree of destruction of the disaster-bearing body are the two most critical indicators, playing an essential role in the evaluation process (Qian et al., 2021). However, with the in-depth study of natural disasters, the importance of social vulnerability has received increasing attention. Apart from hazard factors, social vulnerability indicators are closely related to natural geography, ecological environment, and social factors (Manoharan, 2023).

Generally speaking, domestic research on the vulnerability of disaster-bearing bodies mainly involves constructing evaluation frameworks and models and adopting different evaluation methods to conduct related research on the vulnerability of disaster-bearing bodies from different temporal and spatial scales (Zhao, 2021). Commonly used evaluation methods include disaster-bearing body vulnerability assessments based on historical data (Liang et al., 2015), evaluation indicators (Zhang et al., 2010), scenario simulation (Liu, 2018), etc. Among them, evaluating disaster-bearing body vulnerability based on evaluation indicators is the most commonly used in quantitative vulnerability research (Xu et al., 2022). After constructing an evaluation index system, methods widely used for index assignment during the evaluation of disaster-bearing body vulnerability mainly include the Analytic Hierarchy Process (AHP) (Wang et al., 2024), entropy method (Jia et al., 2023), principal component analysis (Zhao et al., 2023), grey correlation (Yu et al., 2024), and recently, machine learning methods such as random forest, genetic algorithm, and neural network have been widely used in the evaluation of disaster-bearing body vulnerability (Shi et al., n.d.). Domestic research on the vulnerability of disaster-bearing bodies is relatively limited, mainly involving vulnerability and risk assessment. For example, Ma et al. (2021) took county-level administrative regions in Gansu Province as the primary evaluation unit, constructed a risk assessment model from three aspects: agricultural drought hazard, exposure, and vulnerability, analyzed the evaluation results, and provided scientific suggestions for drought prevention and control. He et al. (2024) took 11 provinces in the Yangtze River Economic Belt as the research object, constructed a social vulnerability assessment model based on the Exposure-Sensitivity-Adaptability (ESA) vulnerability assessment framework, and adopted the entropy weight method and multi-level fuzzy comprehensive evaluation method to evaluate and analyze the social vulnerability and spatial-temporal distribution characteristics of flooding in the Yangtze River Economic Belt. Mei (2012) considered the vulnerability of disaster-bearing bodies in the tailings dam collapse area, constructed an evaluation index system for the vulnerability of disaster-bearing bodies, including population, buildings, and roads,

and evaluated the degree of risk loss of disasters such as population and economy. Pei et al. (2017) selected indicators such as population, economy, roads, farmland, medical care, and fiscal revenue and established an evaluation index system for geological disaster exposure, vulnerability, and disaster prevention and mitigation capabilities based on the Analytic Hierarchy Process, and evaluated the vulnerability and risk in Gansu Province. Gao et al. (2018) proposed an index weighting method based on the cloud and natural disaster risk level assessment models. Subsequently, Zhong et al. (2019) combined the cloud-based information diffusion model with the Analytic Hierarchy Process to propose a new mountain flood risk assessment model. This article adopts subjective and objective weighting methods, with the Analytic Hierarchy Process as the subjective method and the cloud model (Jia, 2014) as the objective method. The advantage of the subjective weighting method is that it provides a structured decision-making process, flexibly reflects subjective opinions, and visualizes and communicates the decision-making process. As an objective weighting method, the cloud model can handle uncertainty and fuzziness, flexibly process complex data, and consider integrating multi-source information. Combining the two methods can fully leverage their respective advantages and improve the accuracy and credibility of decision-making.

2. Overview of the Study Area

Yi Ning County is located in the central part of Yi li Valley in the north of Xinjiang Uygur Autonomous Region of China, with a geographical coordinate range of 81°13′4″-82°42′2″E and 43°35′1″-44°29′3″N. It is adjacent to Ni Le Ke County in the east, Ili City and Huo Cheng County in the west, Ili River, Cha Buchar County, Gong Liu County in the south, and Ke Ku Er Qin Mountain in the north. Ku Se Mu Qi Ke River Bole City and Jing he City of Bortala Mongolian Autonomous Prefecture border it. The terrain of Yi Ning County is high in the north and low in the south, mainly divided into three geomorphic units: mountains, hills, and plains. The northern part of the county is mountainous, including Ke Ku Er Qin Mountain and other mountains, with a higher terrain. The central part is hilly, with a relatively lower terrain. The southern part is Ili Valley Plain, with a flatter terrain. From the perspective of the impact of terrain on disasters, there are some potential disaster risks in Yi Ning County. First, it is located on the edge of the seismic active zone in Xinjiang, where earthquakes occur frequently, which may trigger disasters such as landslides, collapses, and ground ruptures, posing potential threats to transportation, residential areas, and farmland. Second, mountainous and hilly terrain is prone to flash floods, and heavy rainfall may lead to floods and mudslides.

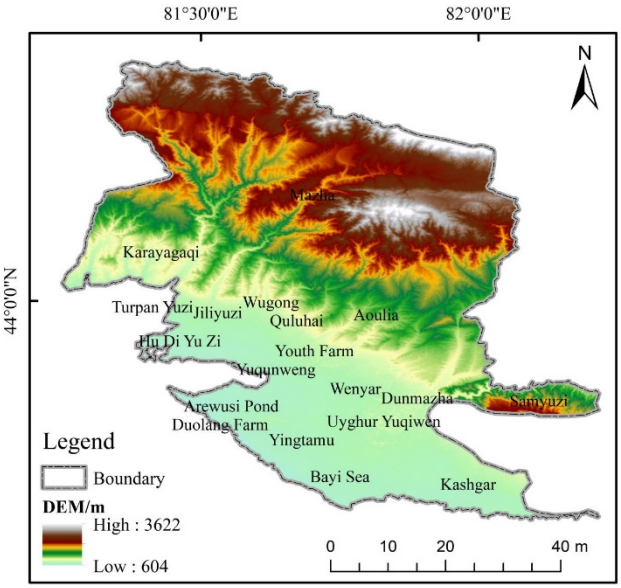

Figure 1. Overview Map of the Study Area

3. Data Source and Processing

The research data primarily originate from the "Leaders' Handbook" and "Statistical Yearbook" of Yi ning County for the years 2005, 2010, 2015, and 2020, including indicators such as permanent resident population, female population, the proportion of elderly and children, total agricultural output value, total industrial output value, grain yield, livestock inventory at the end of the year, and per capita income of farmers and herdsmen. Some indicators require simple calculations, such as population growth rate and transportation facility density. GDP data were obtained from the Resource and Environmental Sciences Data Center of the Chinese Academy of Sciences, road network data were sourced from the National Geomatics Center of China, and POI (Points of Interest) data were collected through web scraping from Gao De Map.

The following standardization process was applied to the 16 indicators of Yi Ning County for the years 2005, 2010, 2015, and 2020. Among the 16 indicators, 14 are positive indicators, while the remaining 2 are negative indicators. Their respective standardization formulas are as follows:

$$x'_{ij} = \frac{x_{ij} - min\{x_{1j}, \cdots, x_{nj}\}}{max\{x_{1j}, \cdots, x_{nj}\} - min\{x_{1j}, \cdots, x_{nj}\}} \quad (1)$$

For indicators with negative functions, the standardization formula is:

$$x'_{ij} = \frac{max\{x_{1j}, \cdots, x_{nj}\} - x_{ij}}{max\{x_{1j}, \cdots, x_{nj}\} - min\{x_{1j}, \cdots, x_{nj}\}} \quad (2)$$

In Equations (1) and (2): represents the value of the j-th indicator in the i-th region（i=1, 2, ⋯n； j=1， 2, ⋯m);x'_{ij} is the normalized value for convenience, in the following calculations, the normalized data is still denoted as x_{ij}.

4. Initial Weight Determination and Optimization Analysis

4.1. Establishment of an Evaluation Index System for Disaster-Bearing Body Vulnerability

Based on the principle of selecting representative indicators, referring to previous research results, and considering the unique characteristics of vulnerability of disaster-bearing bodies in Yi ning County, 16 representative evaluation indicators for meteorological disaster vulnerability assessment have been selected from the three dimensions of population-economy-society. Specifically, the indicators for population vulnerability include the number of permanent residents, the number of female residents, the proportion of elderly and children, and the population growth rate. The indicators for economic vulnerability encompass the GDP of Yi Ning County, the POI (Points of Interest) density in Yi Ning County, the total agricultural output value, the total industrial output value, grain yield, livestock inventory at the end of the year, and the per capita net income of farmers and herders. The indicators for social vulnerability consist of the number of schools, the area of built-up areas, road density, railway density, and transportation facility density. An evaluation index system for meteorological disaster vulnerability assessment encompassing population-economy-society has been constructed, as shown in Table 1.

Table 1. Vulnerability Assessment Indicator System

Objective Level	Criterion Level	Index Level	Nature of the Index
Vulnerability of Disaster-affected Bodies A	Vulnerability of Population A1	Resident Population (people) A11	Positive
		Number of Female Population (people) A12	Positive
		The proportion of the Elderly and Children Population (%) A13	Positive
		Population Growth Rate (%) A14	Positive
	Economic Vulnerability A2	GDP (ten thousand yuan) A21	Positive
		POI Density (%) A22	Positive
		Total Agricultural Output Value (yuan) A23	Positive
		Total Industrial Output Value (yuan) A24	Positive
		Grain Output (tons) A25	Positive
		Number of Livestock at the End of the Year (heads) A26	Positive
		Per Capita Income of Farmers and Herdsmen (yuan) A27	Negative
	Social Vulnerability A3	Number of Schools (units) A31	Negative
		Built-up Area (km^2) A32	Positive
		Highway Density (km/km^2) A33	Positive
		Railway Density (km/km^2) A34	Positive
		Density of Transportation Facilities (units/km^2) A35	Positive

4.2. Determination of Initial Weights

The initial weights are calculated using the Analytic Hierarchy Process (AHP). This paper collects evaluation data from 20 experts. It utilizes the judgment matrix to determine the weights of each indicator, which can reduce the subjectivity and speculation of the decision-maker during the decision-making process(Sun et al., 2023). The calculation steps are as follows:

Step 1: Construct the judgment matrix A.

$$\mathrm{A_{n\times n}} = \left(a_{\mathrm{ij}}\right)_{\mathrm{n\times m}} = \begin{pmatrix} a_{11} & \cdots & a_{1n} \\ \vdots & \ddots & \vdots \\ a_{n1} & \cdots & a_{nn} \end{pmatrix} \quad (3)$$

Wherein: $a_{ij} > 0$; $a_{ij} = \frac{1}{a_{ij}} (i \neq j, i, j = 1,2, \cdots, n)$; $a_{ij} = 1 (i = j, i, j = 1,2, \cdots, n)$.

Step 2: Construct the anti-symmetric matrix B of A based on b_{ij}.

$$b_{ij} = \log a_{ij} \quad (4)$$

Step 3: Obtain the quasi-optimal transitive matrix C based on matrix B.

$$C_{ij} = \frac{1}{n} \sum_{k=1}^{n} (b_{ik} - b_{ik}) \quad (5)$$

Step 4: Construct an optimized consistent matrix A^* according to equation 4.

$$a_{ij}^* = 1c_{ij} \quad (6)$$

Step 5: Calculate the weights of the matrix sing the geometric mean method. This involves taking the product of each row's elements and the square root. Finally, normalizing the results to obtain the initial weights W_{ij}. The indicator weight information obtained from the 20 experts' scores are organized in the following Table 2.

Table 2. Initial Weight Information Table

Indicator	Initial Weight Range	Indicator	Initial Weight Range
A11	0.6≪w_11≪0.95	A25	0.28≪w_25≪0.8
A12	0.29≪w_12≪0.75	A26	0.3≪w_26≪0.7
A13	0.55≪w_13≪0.85	A27	0.1≪w_27≪0.4
A14	0.15≪w_14≪0.6	A31	0.4≪w_31≪0.8
A21	0.29≪w_21≪0.8	A32	0.28≪w_32≪0.6
A22	0.7≪w_22≪0.94	A33	0.4≪w_33≪0.78
A23	0.58≪w_23≪0.85	A34	0.1≪w_34≪0.6
A24	0.3≪w_24≪0.78	A35	0.28≪w_35≪0.8

4.3. Optimization of Weights Based on Cloud Model

4.3.1. Basic Theory of Cloud Model

Li Deyi et al. (Liu, 2010) pioneered the new idea of membership cloud in fuzzy set theory, laying a cornerstone for disseminating and developing cloud theory in social and natural sciences. The membership cloud is an extended theory based on fuzzy set theory used to handle uncertain information. It extends the traditional membership function to a membership cloud function, introducing the concepts of randomness and fuzziness. The working principle diagram of the cloud model (Figure 2) is as follows:

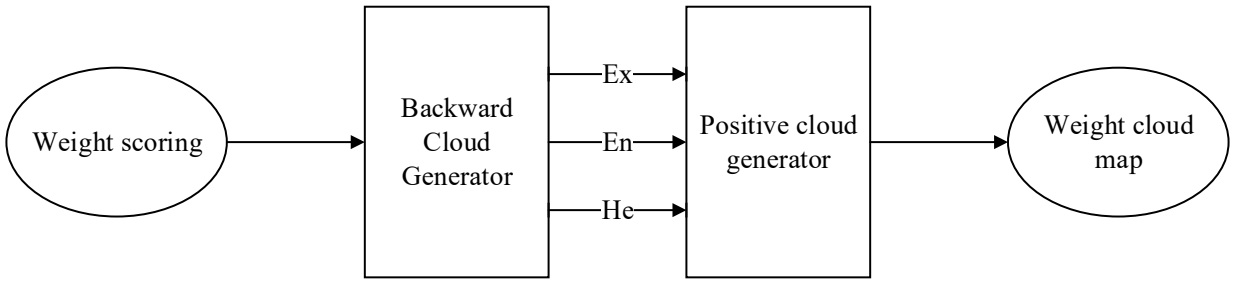

Figure 2. Working Principle Diagram of Cloud Model

4.3.2. Generating Standard Cloud Chart

Based on the qualitative language descriptions provided by disaster-bearing body vulnerability assessment experts regarding the influence intensity of risk assessment indicators, the weight levels are divided into five grades: not necessary, secondarily important, generally important, relatively important, and significant. Given the limited number of evaluation experts and the inability to obtain significant data, this paper adopts the golden section method to divide the weight range (Guo, 2018). As shown in Table 3, the higher the grade, the greater the weight of the corresponding indicator.

Table 3. Numerical Range of Indicator Weight Grades

Weight range	0~0.2	0.2~0.4	0.4~0.6	0.6~0.8	0.8~1
Intensity level Level	1 Level	2 Level	3 Level	4 Level	5 Level
Description	Not important	Somewhat important	Average Importance	Relatively important	Very important
Expected value	0	0.3	0.5	0.7	1
Entropy	0.17	0.33	0.33	0.33	0.17
Super entropy	0.5	0.5	0.5	0.5	0.5

The weight evaluation values such as "secondary importance", "general importance", "significant importance" $[Z_{min}, Z_{max}]$ have bilateral constraints, and the digital characteristic formula for the standard cloud with bilateral constraints are:

$$\mathrm{E_x} = \frac{(Z_{max} + Z_{min})}{2} \tag{7}$$

$$\mathrm{E_n} = \frac{(Z_{max} - Z_{min})}{6} \tag{8}$$

$$\mathrm{H_{e=}}c \tag{9}$$

In the equation, c is a constant, and the hypertrophy can be adjusted and utilized based on its fuzziness. Here, c is taken as 0.5. The forward cloud generator constructs the standard cloud chart (Figure 3) for evaluating the weight of indicators in MATLAB software, serving as a benchmark reference for determining the weight of indicators.

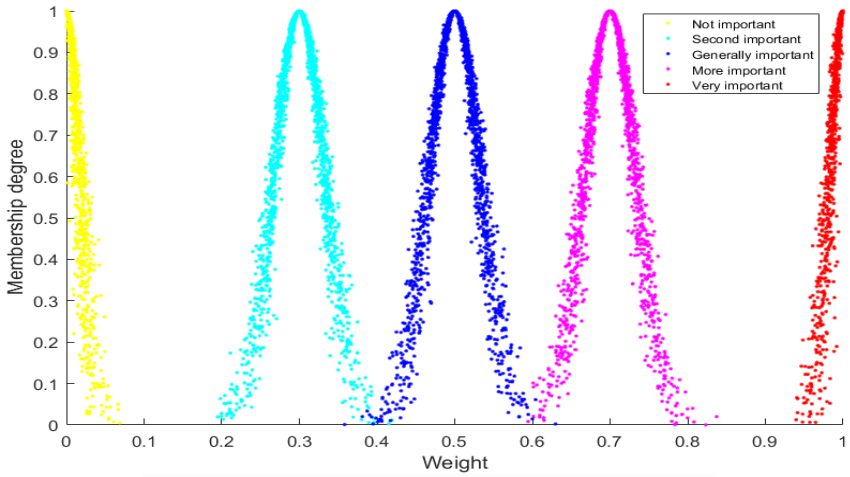

Figure 3. Standard Cloud Chart for Indicator Weights

4.3.3. Generating the Cloud Model for the Final-level Indicator Weights

Using the Analytic Hierarchy Process (AHP), initial weights for the indicators are formed, and the cloud model is utilized to refine and rationalize the weights continuously. The reverse cloud generator algorithm is employed to generate the numerical characteristics of the cloud model, and then the forward cloud generator is used to produce the cloud chart. The first round of scoring results is fed back to the experts, who then conduct a second round of scoring. This process is repeated multiple times until the cloud chart converges from a foggy state to a condensed one. To maintain the randomness and uncertainty of the experts' evaluations, the reverse cloud generator is used to derive the three characteristic values of the cloud model, and then the forward cloud generator generates the cloud chart. The specific process is illustrated in Figure 4 (Zhong, 2014).

$$\mathrm{E_x} = \bar{x} \tag{10}$$

$$\mathrm{E_n} = \sqrt{\frac{\pi}{2}}\frac{1}{n} \tag{11}$$

$$H_e = \sqrt{\frac{1}{n}\sum_{i=1}^{n}(x_i - \bar{x})^2 - En^2} \tag{12}$$

Based on the forward cloud generator algorithm, the weight cloud chart of the first scoring round is obtained, which appears foggy. The conceptual ambiguity CD calculated according to formula (13) equals 1, indicating that the experts' understanding of the concept of indicator weights is divergent, and it is not easy to reach a consensus. During the second round of consultation, the information from the first round of expert scoring is filtered, classified, and summarized for feedback to the experts. The experts then adjust their scoring results based on the opinions of multiple experts. The hyper-entropy and entropy of the cloud model in the second round of scoring are significantly smaller than those in the first round, and the cloud chart no longer appears "foggy," as shown in Figure 4. The cloud chart begins to condense from a misty state, indicating that the concept of the importance of indicators is starting to form. In the third round of scoring, the hyper-entropy and entropy of the cloud model further decrease, and the thickness of the cloud becomes significantly thinner, enhancing the condensation of the cloud chart again. As shown in the figure, the conceptual ambiguity CD is equal to 0.4153, indicating that the concept of the importance of indicators is relatively mature (Liu et al., 2009).

$$\mathrm{CD} = \frac{3\mathrm{He}}{\mathrm{En}} \tag{13}$$

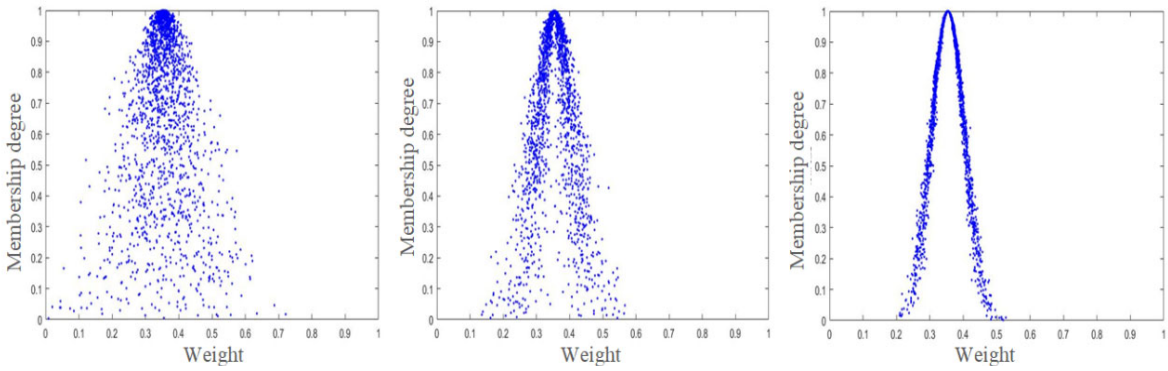

Figure 4. Aggregation Process of the Cloud Chart for Index Weight

By repeating the first and second steps, we finally obtained the numerical characteristics and fuzziness of the cloud model for the weights of 16 indicators, as shown in Table 4. The fuzziness of all 16 indicators falls within the range of (0.2, 0.544], indicating that experts hold relatively consistent views on the weight results of these 16 indicators, forming a more mature concept.

Table 4. Numerical Characteristics and Fuzziness of the Cloud Model for the Indicator System

Target level	Criteria level	Cloud model	Degree of fuzziness	Indicator level	Cloud model	Degree of fuzziness
A	A1	C(0.674,0.0806,0.0059)	0.2196	A11	C(0.84,0.0353,0.0048)	0.4152
				A12	C(0.65,0.0332,0.0053)	0.4847
				A13	C(0.74,0.043,0.0061)	0.4275
				A14	C(0.47,0.0375,0.0056)	0.454
	A2	C(0.572,0.0995,0.0047)	0.1417	A21	C(0.89,0.0322,0.0048)	0.4006
				A22	C(0.68,0.0344,0.0054)	0.4787
				A23	C(0.6,0.0367,0.0054)	0.4413
				A24	C(0.4,0.0355,0.0049)	0.4141
				A25	C(0.57,0.0331,0.0055)	0.4984
				A26	C(0.16,0.0286,0.0048)	0.5094
				A27	C(0.7,0.0335,0.0049)	0.4152
	A3	C(0.372,0.0934,0.0048)	0.1541	A31	C(0.26,0.0352,0.0042)	0.3579
				A32	C(0.48,0.0284,0.0042)	0.4496
				A33	C(0.62,0.0299,0.0044)	0.4417
				A34	C(0.17,0.0286,0.0046)	0.4919
				A35	C(0.35,0.0348,0.0046)	0.4919

4.3.4. Generating the Cloud Model for High-level Indicator Weights

The comprehensive cloud, also known as the parent cloud, essentially elevates the concept by integrating linguistic values of the same type into a more generalized concept with a broader meaning, resulting in a higher-level parent cloud. In the indicator system, high-level indicators represent concepts of higher comprehensiveness, which aligns with the essence of the comprehensive cloud. Therefore, secondary indicators can be considered the parent cloud of tertiary indicators, and primary indicators can be seen as the parent cloud of secondary indicators. The numerical characteristics of the comprehensive cloud can be calculated based on the numerical attributes of all its sub-clouds, as shown in the calculation formulas (14), (15), and (16).

$$E_{x'} = \frac{E_{x_1} \times E_{n_1} + E_{x_2} \times E_{n_2} + \cdots + E_{x_k} \times E_{n_k}}{E_{n_1} + E_{n_2} + \cdots + E_{n_k}} \quad (14)$$

$$E_{n'} = E_{n_1} + E_{n_2} + \cdots + E_{n_k} \quad (15)$$

$$H_{e'} = \frac{H_{e_1} \times E_{n_1} + H_{e_2} \times E_{n_2} + \cdots + H_{e_k} \times E_{n_k}}{E_{n_1} + E_{n_2} + \cdots + E_{n_k}} \quad (16)$$

The weighted average method adopted for the numerical characteristic value Ex of the cloud model for all weight evaluation indicators can more reasonably and comprehensively reflect the weight of the indicators. By normalizing the weights of indicators at the same level according to formula (17), we can obtain the final weight values of the indicator system, achieving a quantitative representation of the weights. The result is shown in Figure 4. A bidirectional cognitive model combining qualitative and quantitative weights can be established through the cloud model, realizing the unity. Based on the Gaussian cloud model of the indicator weights, we can calculate its average membership degree at each evaluation level and determine the qualitative weight level to which the indicator belongs according to the principle of maximum membership degree.

$$W_i = \frac{E_{x_i}}{\sum_{i=1}^{n} E_{x_i}} \quad (17)$$

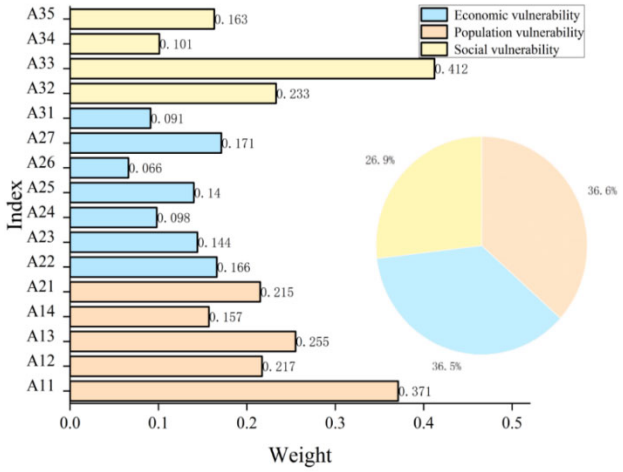

Figure 5. Histogram of Indicator Weights

The histogram of weight distribution reveals that the proportion of the elderly and young population and population growth rate are assigned higher weights regarding population vulnerability, indicating that population structure plays a significant role in vulnerability assessment. High levels of aging and youthfulness may increase social demands, resource pressure, and the need for social security, thus enhancing vulnerability. High population growth rates may

lead to increased resource consumption and pressure on socio-economic development, contributing to vulnerability. GDP and POI density are more critical regarding economic vulnerability, indicating that the financial scale and economic activity centers significantly impact vulnerability assessment. The total agricultural output, food production, and livestock inventories are assigned lower weights, suggesting that agriculture and animal husbandry have a relatively minor influence on vulnerability assessment. Total agricultural output and food production are related to rural residents' income, but their importance in the overall evaluation is relatively low. Regarding social vulnerability, roads, and construction land occupy a higher proportion, mainly because the connectivity and resilience of the road network are crucial to society's resilience and response capabilities. Low road network density or poor road quality may lead to traffic paralysis during disasters, hindering rescue and emergency response. Large-scale construction land may imply more population and social activities but also increase disaster risks and exposure. If the construction land is located in disaster-prone areas or high-risk zones, vulnerability may increase.

5. Analysis of Spatial and Temporal Characteristics of Disaster-bearing Body Vulnerability

In ArcGIS, the weights obtained from the cloud model and the standardized indicator data are substituted into formula (18) for weighted comprehensive calculation. The disaster-bearing body's population, economic, social, and comprehensive vulnerability are divided into five grades using the natural breaks method in ArcGIS tools to facilitate observation.

$$H_j = \sum_{i=1}^{n} w_i x_{ij} \tag{18}$$

Where: H_j represents the indicator evaluation index, w_i represents the weight value of the indicator, and $represents$s the standardized data of the indicator.

5.1. Analysis of Spatial and Temporal Characteristics of Population Vulnerability

In combination with the population size and the contribution of population age structure to population vulnerability, spatially speaking, the population vulnerability in Yi Ning County is influenced by the terrain, showing a general trend of being lower in the north and higher in the south. The northern region is mainly mountainous and hilly, while the southern region is primarily plain with a high population density, making it the main area with high population vulnerability. Looking specifically at the indicators of population vulnerability, there are spatial differences in the vulnerability of each township and its contributing factors. First, Ji Li Yu Zi, Yu Qun Weng Hui Ethnic Township, Wen Ya Er Township, and Ying Ta Mu Township have consistently high or above-average annual vulnerability levels. The main reason is that these four townships have a dense population, exposing a large group to disasters. Second, several townships on the fringes of high vulnerability have lower populations than high-vulnerability townships, such as Ba Yi Tuo Hai Township, Are Wu Si Tang Township, Hu Di Yu Zi Township, etc. However, Ma Zha Township, located in the mountainous and hilly area in the north, has consistently remained at a low level of vulnerability. Third, some townships have undergone significant changes. For example, A Wu Li Ya Township has shifted from low to higher vulnerability, while Ka Shi Township has shifted from medium to low vulnerability. These changes are mainly due to significant changes in their population sizes between 2015 and 2020.

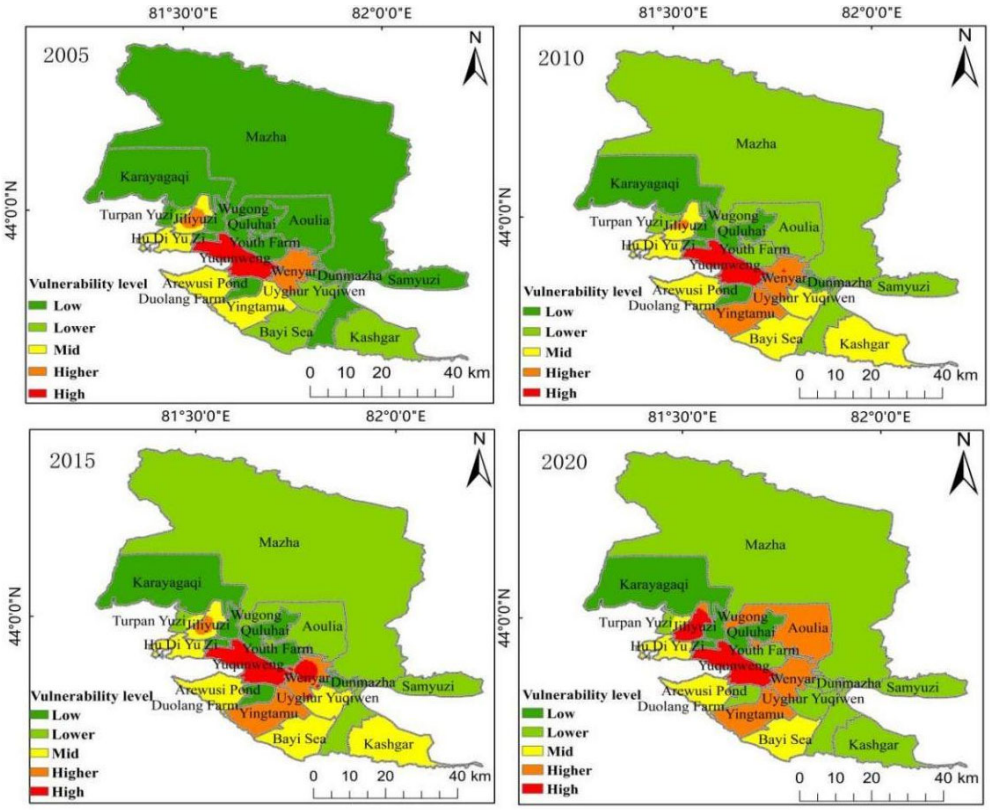

Figure 6. Spatial Distribution of Population Vulnerability in Different Years

Over time, the overall population vulnerability in Yi Ning County has shown an increasing trend, with a continuous growth in population from 2005 to 2020. According to reliable population statistics, the population of Yi Ning County was 371,800 in 2005. Yi Ning County experienced rapid socioeconomic development and urbanization as time progressed, attracting more migration. By 2010, the population of Yi Ning County had increased to 426,800, representing a significant growth compared to 2005. This growth trend continued to strengthen in the following years, reaching 582,700 in 2020, maintaining a stable growth momentum. Over time, the population structure of Yi Ning County has also changed, with a gradual increase in the proportion of the elderly and young population. From 2005 to 2020, the proportion of the elderly population in Yi Ning County gradually increased, reflecting the trend of population aging. Observing the graph, it can be seen that from 2005 to 2010, the proportion of areas with low population vulnerability in Yi Ning County decreased from 60.09% to 13.88%, while the proportion of regions with relatively low vulnerability increased from 18.76% to 62.16%, showing a significant mutation. Between 2010 and 2020, there were some fluctuations but no significant overall trend. The proportion of areas with high vulnerability increased slowly from 2.83% to 4.81% from 2005 to 2015 and then increased significantly to 6.3% in 2020. This indicates changes in some indicators that affect population vulnerability, such as population growth and the aging and feminization of the age structure.

Table 5. Area and Proportion of Population Vulnerability Levels in Different Years

	2005		2010		2015		2020	
Vulnerability Level	Area (km²)	Proportion (%)	Area (km²)	Proportion (%)	Area (km²)	Proportion (%)	Area (km²)	Proportion (%)
Low	24857	6.9	558	13.88	5971	14.36	485	11.14
Lower	7185	18.76	24658	62.16	2559	61.44	25514	65.65
Mid	6691	16.18	5543	14.81	5899	15.18	2781	7.16
Higher	833	2.14	253	5.18	221	4.21	4178	9.75
High	111	2.83	1542	3.97	197	4.81	265	6.3

5.2. Analysis of Spatial and Temporal Characteristics of Economic Vulnerability

The distribution of economic vulnerability and its dominant factors showed significant spatial and temporal differences from 2005 to 2020. Firstly, Ma Zha Township, Ka La Ya Ga Qi Township, Wu Gong Township, Qu Lu Hai Township, and A Wu Li Ya Township remained at a low level of vulnerability throughout the years. The main reason is that most of these townships are in mountainous and hilly areas with high altitudes and rugged terrain, making economic infrastructure construction difficult. The mountainous terrain often limits land use, posing challenges to agricultural development. Steep slopes and irregular terrain hinder large-scale mechanized agriculture. The lack of flat land and large-scale industrial parks makes it difficult to establish large enterprises. Secondly, Ji Li Yu Town, Yu Qun Weng Hui Township, Wen Ya Er Township, Ying Ta Mu Township, and Ba Yi Tuo Hai Township exhibited high vulnerability. This is mainly due to the flat plains in the south, with rapid urbanization and economic growth. The flat land facilitates irrigation and water conservancy facilities, providing sufficient crop water sources. This contributes to increased agricultural yields and diversified crop cultivation. It also enables industrial development, more accessible industrial parks and factory construction, high land utilization rates, and relatively low construction costs. Additionally, it provides vast grasslands and pastures for animal husbandry, allowing herders to graze and manage livestock conveniently. From a temporal perspective, between 2005 and 2020, the proportion of low vulnerability remained relatively stable, fluctuating between 68.97%, 69.2%, 66.1%, and 69.9%. The proportion of relatively low vulnerability was also stable, ranging from 3.24%, 6.81%, 3.3%, and 3.16%. The proportion of moderate vulnerability gradually decreased from 22.37% in 2005 to 4.32% in 2022. Meanwhile, the proportion of relatively high vulnerability gradually increased from 2.41% in 2005 to 15.13% in 2020. High vulnerability gradually increased from 3.1% in 2005 to 8.3% in 2020. Overall, the proportion of moderate vulnerability decreased, while the proportion of relatively high and high vulnerability gradually increased.

In summary, from 2005 to 2020, the area and proportion of moderate vulnerability decreased, while the area and proportion of relatively high and high vulnerability increased. This may indicate that regions with lower overall vulnerability remained stable during this period, while areas with higher vulnerability increased.

Table 6. Area and Proportion of Economic Vulnerability Levels in Different Years

	2005		2010		2015		2020	
Vulnerability Level	Area (km²)	Proportion (%)	Area (km²)	Proportion (%)	Area (km²)	Proportion (%)	Area (km²)	Proportion (%)
Low	25169	68.97	25255	69.2	24123	66.1	25142	69.9
Lower	1184	3.24	2486	6.81	124	3.3	115	3.16
Mid	8157	22.37	5643	15.36	3398	9.31	339	4.32
Higher	881	2.41	211	5.51	6254	17.14	555	15.13
High	13	3.1	1199	3.12	1515	4.15	221	8.3

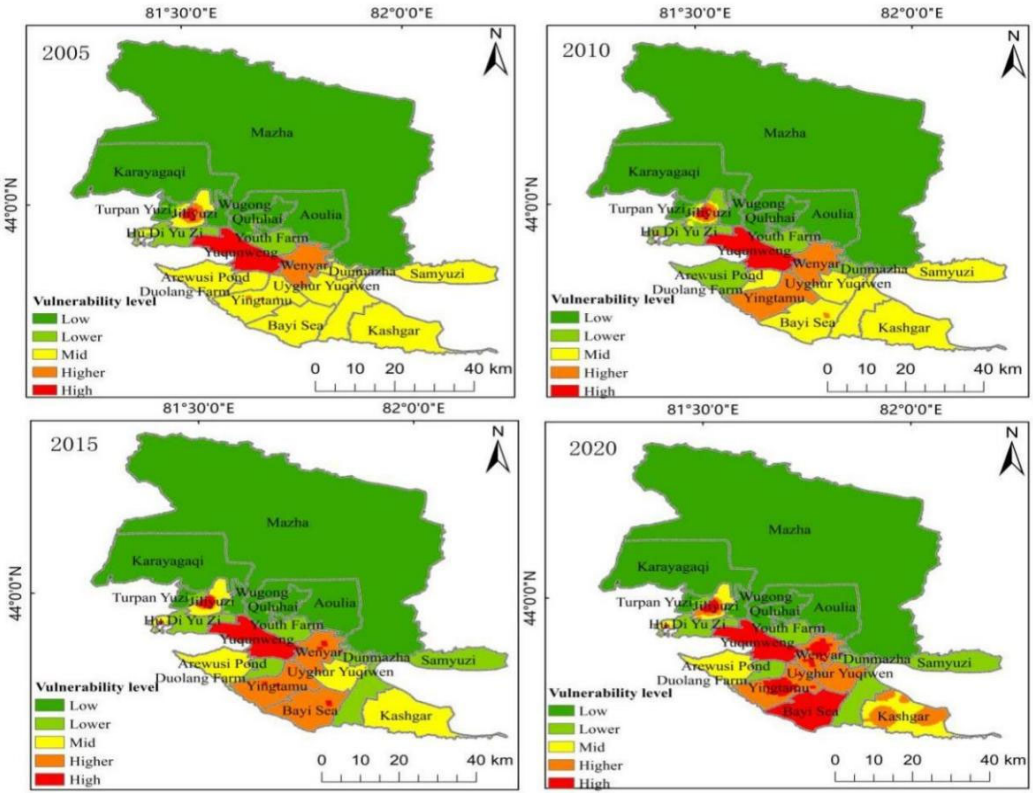

Figure 7. Spatial Distribution of Economic Vulnerability in Different Years

5.3. Analysis of Spatial and Temporal Characteristics of Social Vulnerability

The figure above demonstrates the spatial and temporal distribution of social vulnerability in Yi Ning County from 2005 to 2020. Regionally, high vulnerability is concentrated in the southern plains with dense road networks and rapid urbanization, such as the areas around Ji li Yu Town-Yu Qun Weng Hui Township and Ba Yi Tuo Hai Township-Wen Ya Er Township. In contrast, the northern mountainous areas, with rugged terrain, face transportation and infrastructure construction challenges. The complexity of the terrain may limit the scale and progress of housing and road construction, resulting in relatively low vulnerability in these regions due to the smaller scale of human activities and related infrastructure.

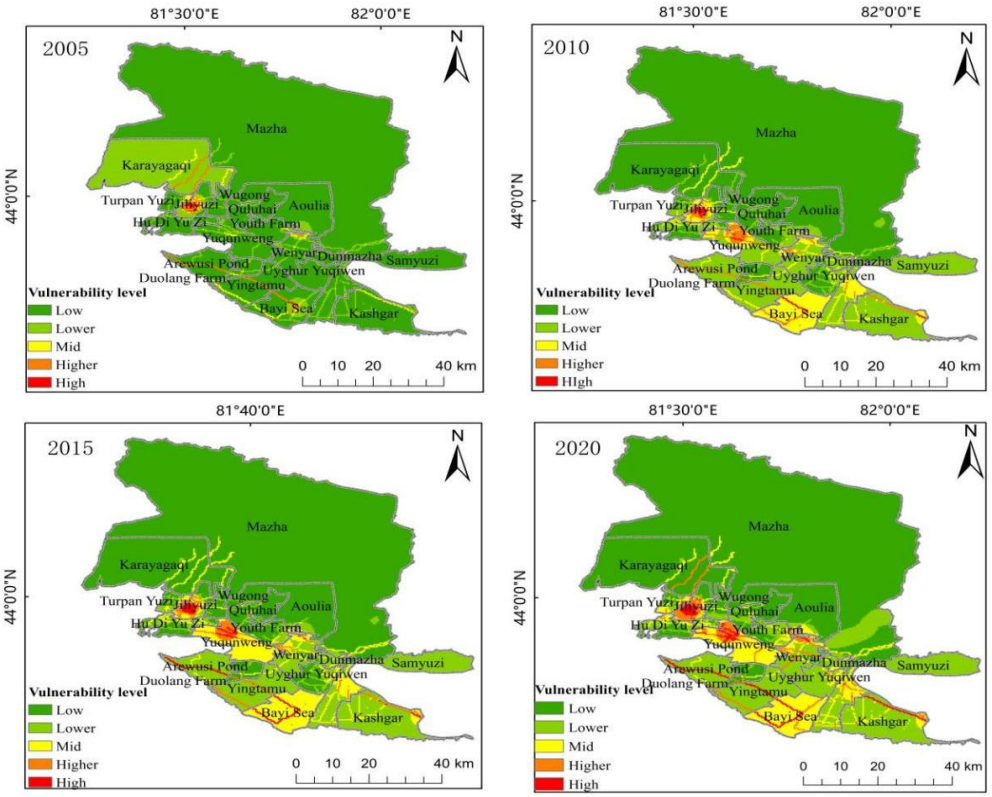

Figure 8. Spatial Distribution of Social Vulnerability in Different Years

From a temporal perspective, between 2005 and 2020, the proportion of low vulnerability gradually decreased from 84.22% to 63.2%. The proportion of relatively low vulnerability peaked in 2015 and then declined but remained high, increasing from 13.53% to 13.22%. The proportion of moderate vulnerability increased between 2010 and 2020, from 1.13% to 1.99%. The proportion of relatively high vulnerability peaked in 2015, rising from 0.93% to 8.44%. The proportion of high vulnerability also peaked in 2015, rising from 0.18% to 4.32%. Overall, the proportion of low vulnerability decreased, while moderate, relatively high, and high vulnerability gradually increased.

From 2005 to 2020, the area and proportion of low vulnerability showed a decreasing trend, while the area and proportion of moderate, relatively high, and high vulnerability exhibited an increasing trend. This suggests that during this period, the area of high-vulnerability regions increased while the area of low-vulnerability regions decreased.

Table 7. Area and Proportion of Social Vulnerability Levels in Different Years

	2005		2010		2015		2020	
Vulnerability Level	Area (km²)	Proportion (%)	Area (km²)	Proportion (%)	Area (km²)	Proportion (%)	Area (km²)	Proportion (%)
Low	32731	84.22	2746	7.52	5971	15.36	22282	63.2
Lower	5259	13.53	6948	17.88	2559	64.48	4674	13.22
Mid	439	1.13	377	9.54	5899	15.18	3886	1.99
Higher	363	0.93	67	1.72	833	2.14	2984	8.44
High	71	0.18	132	0.34	111	2.83	1529	4.32

5.4. Analysis of Spatial and Temporal Characteristics of the Comprehensive Vulnerability of Disaster-Bearing Bodies

By combining population, economic, and social vulnerability, this analysis examines explicitly the causes of the comprehensive vulnerability of meteorological disaster-bearing bodies in Yi Ning County. According to the histogram of weight distribution, it can be observed that population and economic factors have a higher proportion and play a decisive role in the comprehensive vulnerability of disaster-bearing bodies in Yi Ning County compared to social factors. Overall, the comprehensive vulnerability of meteorological disaster-bearing bodies is higher in the south and lower in the north. Towns in the southern part of Yi Ning County, such as Ji Li Yu Town, Yu Weng Qun Hui Township, Wen Ya Er Township, Ying Ta Mu Township, and Ba Yi Tuo Hai Township, have a high population density, sound economic development, and rapid urbanization, resulting in high vulnerability. Conversely, towns like Ma Zha Township and Ka La Ya Ge Qi Township have lower comprehensive vulnerability. These townships may have a lower population density, relatively weak economic development, and slower urbanization. The lower population density may reduce casualties and safety risks, the relatively weak economic growth may result in less impact from meteorological disasters, and the slower urbanization process may give townships more time to adapt and prepare for disasters.

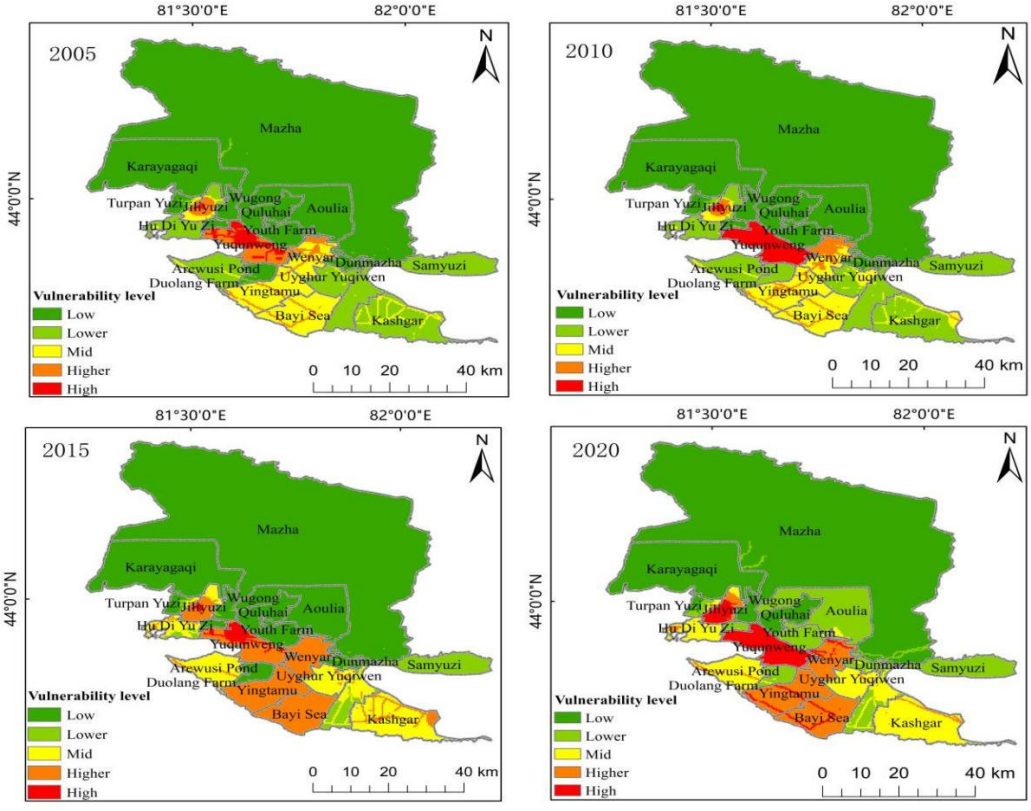

Figure 9. Spatial Distribution of the Comprehensive Vulnerability of Disaster-Bearing Bodies in Different Years

From a temporal perspective, from 2005 to 2020, the proportion of low vulnerability gradually decreased from 72.45% to 63.2%. The proportion of relatively low vulnerability reached its lowest point in 2015 and then increased but remained at a low level, rising from 5.36% to 13.22%. The proportion of moderate vulnerability increased in 2015 and then decreased in 2020, from 12.45% to 1.99%. The proportion of relatively high vulnerability showed a significant increase in 2015 and then reduced in 2020, rising from 1.9% to 8.44%. The proportion of high vulnerability increased significantly in 2010 and then slightly reduced, from 1.37% to 4.33%. From 2005 to 2020, the area and proportion of low vulnerability reduced somewhat, while the area and proportion of relatively low, moderate, high, and high vulnerability fluctuated. This may indicate an overall increase in the vulnerability of meteorological disaster-bearing bodies during this period.

Table 8. Area and Proportion of Comprehensive Vulnerability Levels of Disaster-Bearing Bodies in Different Years

	2005		2010		2015		2020	
Vulnerability Level	Area (km^2)	Proportion (%)	Area (km^2)	Proportion (%)	Area (km^2)	Proportion (%)	Area (km^2)	Proportion (%)
Low	32731	84.22	2746	7.52	5971	15.36	22282	63.2
Lower	5259	13.53	6948	17.88	2559	64.48	4674	13.22
Mid	439	1.13	377	9.54	5899	15.18	3886	1.99
Higher	363	0.93	67	1.72	833	2.14	2984	8.44
High	71	0.18	132	0.34	111	2.83	1529	4.32

6. Conclusions and Recommendations

This paper assessed meteorological disaster-bearing bodies at the township level in Yi Ning County by establishing a vulnerability evaluation index system for meteorological disasters and utilizing the AHP-cloud model weight determination model. Based on the analysis of the assessment results, the following conclusions were drawn:

(1) Demographic structure, economic factors, and social factors significantly impact the vulnerability assessment of meteorological disaster-bearing bodies in Yi Ning County. High aging and infantilization, as well as high population growth rates, exacerbate the vulnerability of disaster-bearing bodies. Meanwhile, economic output, road networks, and construction land significantly influence social vulnerability.

(2) The population vulnerability in Yi Ning County is significantly influenced by the terrain, showing an overall trend of being lower in the north and higher in the south. Due to their high population density, the southern plain areas have become the main areas with high population vulnerability. During the period from 2005 to 2020, the population of Yi Ning County continued to grow, and the proportion of the elderly population gradually increased, leading to an overall increasing trend in population vulnerability.

(3) The economic and social vulnerability of Yi Ning County showed significant spatial and temporal differences from 2005 to 2020. Mountainous and hilly areas had a lower economic vulnerability, while the southern plain regions had a higher economic vulnerability due to rapid urbanization and abundant resources. Regarding social vulnerability, the south plain areas were concentrated areas of high vulnerability, while the northern mountainous regions had relatively lower vulnerability. Overall, the comprehensive vulnerability of meteorological disaster-bearing bodies in Yi Ning County is dominated by population and economic factors, with higher vulnerability in the southern and lower vulnerability in the northern townships. Over time, the vulnerability of disaster-bearing bodies has increased. To reduce the vulnerability of meteorological disaster-bearing bodies in Yi Ning County and enhance its disaster reduction capabilities, the following recommendations are proposed:

(1) Management of demographic factors: Considering the impact of high aging and infantilization rates on vulnerability, appropriate population policies should be formulated to promote balanced development in population structure. Welfare security for older people and children should be strengthened, and proper medical, educational, and social service facilities should be provided.

(2) Economic development: Focus on developing the economy in mountainous and hilly areas, overcoming geographical constraints and infrastructure construction difficulties, and enhancing economic vitality. Urbanization should be planned and managed rationally in the southern plain regions to ensure the sustainability of economic development and resource utilization.

(3) Improvement of social factors: Strengthen road network construction, improve transportation connectivity and disaster resistance capabilities, and facilitate rapid response and rescue during disasters. Plan and manage construction land rationally to ensure a balanced distribution of social infrastructure and improve communities' resilience to disasters.

References

[1] Gao YQ, Chen HY, Liu YP. (2018). Assessment of Disaster Severity of Natural Disasters Based on Cloud Model. Advances in Science and Technology of Water Resources, 38(6), 38-43+60.

[2] Guo X. (2018). Research on Index Weight of Logistics Integration in Beijing-Tianjin-Hebei Based on Cloud Model. Journal of Yunnan University of Finance and Economics, 34(6), 96–104. https://doi.org/10.16537/j.cnki.jynufe.000326

[3] He L, Chen JC, Cheng CG. (2024). Social Vulnerability Assessment and Spatial-Temporal Analysis of Flood Disasters in the Yangtze River Economic Belt. Water Resources and Hydropower Engineering (Chinese and English), 1–16.

[4] Jia XL, Xu JL. (2014). Earthquake Risk Assessment of Highway in Earthquake Area Based on Cloud Model. Journal of Tongji University (Natural Science Edition), 42(9), 1352-1358+1458.

[5] Jia YH, Bai Y, Zhai LX. (2023). Risk Assessment of Rainstorm and Flood Disasters in Guangxi Based on AHP-Entropy Weight Method. Surveying and Spatial Geographic Information, 46(10), 13–17.

[6] Liang HQ, Xia BC, Liu DL. (2015). Review of Vulnerability Research on Natural Disasters. North China Earthquake Sciences, 33(1), 11–18.

[7] Liu Y, Li DY, Zhang GWi.(2009). Nebulization Characteristics of Cloud Model and Its Application in Evolutionary Algorithms. Acta Electronica Sinica, 37(8), 1651–1658.

[8] Liu Y, Li DY. (2010). Statistical Analysis of Normal Cloud Model Nebulization Properties. Journal of Beijing University of Aeronautics and Astronautics, 36(11), 1320–1324. https://doi.org/10.13700/j.bh.1001-5965.2010.11.026

[9] Liu ZZ. (2018). Vulnerability Analysis of Urban Community Waterlogging Disaster from the Perspective of Scenario Simulation. China Public Safety (Academic Edition), 2, 53–56.

[10] Ma MM, Meng ZX. (2021). Research on the Risk Assessment of Agricultural Drought Based on the Theory of Regional Disaster System: A Case Study of Gansu Province. China Flood and Drought Management, 31(S1), 75–78.

[11] Manoharan, Ganapathy.(2023). GIS-based urban social vulnerability assessment for liquefaction susceptible areas: A case study for greater Chennai, India. Geoenvironmental Disasters, 10(1), 1. https://doi.org/10.1186/s40677-022-00230-5

[12] Mei G, Wu Z. (2012). Research on the Dam-Break Hazard Vulnerability Assessment Index System and Methods of Tailings Pond. Applied Mechanics and Materials, 204–208, 3450–3456. https://doi.org/10.4028/www.scientific.net/AMM.204-208.3450

[13] Mei GD. (2012). Research on the Vulnerability Assessment Index System and Methods of Tailings Pond Dam Break Disaster. China Safety Science Journal (12), 11-15.

[14] Pei HJ, Chen J, Li W. (2017). Geological Disaster Risk Assessment in Gansu Province. Journal of Catastrophology, 32(2), 97–102.

[15] Qian HW, Liu C, Wang JD. (2021). Discussion on Related Concepts of Disaster Vulnerability. Safety, 42(7), 45-49+55+5. https://doi.org/10.19737/j.cnki.issn1002-3631.2021.07.008

[16] Shi XL, Zhang Y. (2024). Research Progress in Natural Disaster Risk Assessment. Journal of Xi'an University of Technology, 1–11.

[17] Sun JF, Ma C, Hu JS. (2023). Geological Disaster Susceptibility Evaluation Based on the Coupling of Grey Relational Analysis and Analytic Hierarchy Process: A Case Study of Chongtou Town, Yunhe County, Zhejiang Province. Journal of Engineering Geology, 31(2), 538–551. https://doi.org/10.13544/j.cnki.jeg.2022-0542

[18] Wang DY, Ji C, Zhang LD. (2024). Multi-Method Combined Assessment and Application of Urban Flood Risk. Journal of Catastrophology, 39(1), 96–103.

[19] Xu W, Liu K, Li BX. (2022). Vulnerability Assessment of Disaster-Bearing Bodies in Major Multi-Disaster Natural Disasters: Indicators, Methods, and Results. China Disaster Relief, 7, 16–18.

[20] Yu Mancang, Lv Dunyu, Meng Shuran. (2024). Research on Risk Assessment of Urban Ground Collapse Disasters. Geology and Prospecting, 60(1), 63–75.

[21] Zhang B, Zhao QS, Jiang YJ. (2010). Research on Vulnerability Index System and Fine Quantification Model of Regional Disaster-Bearing Bodies. Journal of Catastrophology, 25(2), 36–40.

[22] Zhao DL. (2021). Comprehensive Evaluation of Vulnerability of Social-Ecological System Disaster-Bearing Bodies on the Qinghai-Tibet Plateau [Master's Thesis, Qinghai Normal University]. https://doi.org/10.27778/d.cnki.gqhzy.2021.000116

[23] Zhao, Liu Q, Zhu J. (2023). Risk Assessment and Zonation of Roof Water Inrush Based on the Analytic Hierarchy Process, Principle Component Analysis, and Improved Game Theory (AHP–PCA–IGT) Method. Sustainability, 15(14), 11375. https://doi.org/10.3390/su151411375

[24] Zhong M, Wang J, Gao L.(2019). Fuzzy Risk Assessment of Flash Floods Using a Cloud-Based Information Diffusion Approach. Water Resources Management, 33(7), 2537–2553. https://doi.org/10.1007/s11269-019-02266-z

[25] Zhong M. (2014). Multi-level Fuzzy Comprehensive Evaluation of Reservoir-induced Earthquake Risk Based on Association Rules and Cloud Model [Doctoral Dissertation, Huazhong University of Science and Technology]. https://kns.cnki.net/kcms2/article/abstract